Copyright ©

Aus dem Institut für Meereskunde an der Universität Kiel

A theory of time-dependent upwelling induced by a spacially- and temporally- varying wind with emphasis on the effects of a seabreeze-landbreeze cycle

By GARY SHAFFER

Eine Theorie des zeitabhängigen, durch räumlich und zeitlich veränderlichen Wind erzeugten Auftriebs, unter besonderer Berücksichtigung der Wirkung des Land-See-Windes (Zusammenfassung): Für einen plötzlich einsetzenden Wind werden Lösungen des Geschwindigkeitsfeldes in einem Modellozean (homogen, unendlich tief und breit, an einer Seite von einer vertikalen Wand begrenzt) abgeleitet. Der Wind setzt sich aus einem Passat und einem periodischen Land-See-Wind zusammen; beide klingen exponentiell mit der Entfernung vom Land ab.

Die Lösungen werden für verschiedene Grenzfälle untersucht. Wegen der Linearität des Modells sind die Lösungen separabel. Für die Zeit $t \to \infty$ ergeben sich 1.) stationäre Aufwärtsbewegungen von ca. 6×10^{-3} cm/sec innerhalb der Küsten-nahen Ekman-Schicht von etwa 50 km Breite und Absinken über die Breite des Passats sowie 2.) horizontale und vertikale Schwingungen mit eintägiger Periode. Bei 20° geographischer Breite betragen die mit ihr verbundenen vertikalen Geschwindigkeiten 0 (10^{-2} cm/sec) innerhalb der Küsten-nahen Ekman-Schicht und 0 (10^{-3} cm/sec) außerhalb.

Die Amplituden der Schwingungen sind breitenabhängig und zeigen eine Resonanz bei 30°, wo die Trägheitsfrequenz und die Frequenz des Land-See-Windes gleich sind. Es wird angenommen, daß der „Überschuß an Wellenenergie" bei 30° dem turbulenten Feld zugeführt wird, woraus erhöhte Vermischung resultieren müßte. Dies kann eine Erklärung für die bei 30° beobachteten Temperatur-Minima sein.

Summary: Solutions are derived for the velocity field of a model ocean — homogeneous, infinitely deep and wide, and bounded on one side by a vertical wall — resulting from a wind which suddenly starts to blow. This model wind consists of a trade wind and a land-seabreeze, both of which decrease exponentially from shore.

These solutions are then analysed for various limiting cases. Due to the linearity of the model, these solutions are separable and yield for $t \to \infty$ 1.) steady-state upwelling of about 6×10^{-3} cm/sec within the coastal Ekman layer of width 0 (50 km) as well as sinking across the width of the trade wind belt and 2.) horizontal and vertical oscilliations of daily period. At 20° the vertical oscillations have amplitudes 0 (10^{-2} cm/sec) within the coastal Ekman layer and 0 (10^{-3} cm/sec) outside of it.

In addition the amplitudes of these oscillations are found to be functions of latitude, exhibiting a resonance point at 30° where the inertial frequency and the land-sea-breeze frequency are the same. It is postulated that the "unbounded" wave energy around 30° is transfered to the turbulent field resulting in increased mixing by 30°. This could possibly explain the relative temperature minima observed there.

1. Introduction

The purpose of this analysis is to examine theoretically the velocity field in an ocean, in the presence of a boundary, called forth by a local wind stress that varies in both space and time. In particular the effect of a seabreeze-landbreeze cycle is to be studied. The upward component of this velocity field is of fundamental importance to the biological production since it enriches the upper layers of the ocean with nutrients in the process known as upwelling. As I choose to define it for this analysis, upwelling is the ascending motion of water into the surface Ekman layer (more biologically significant: into the euphotic zone) from the layers below it. This should be understood as a net motion whereby the periodic motions are eliminated by appropriate averaging.

This undertaking was motivated by observations made in the regions of coastal upwelling. Such observations whether they be made from research vessels, from

coastal stations, or from planes or satellites by means of infra-red temperature measurements, underline the variability of the velocity field. It is hoped that the results of this study will contribute to the understanding of this variability.

The variability can be periodic (ex. internal waves, tides, the effect of a periodic wind), non-periodic (ex. changes in the weather), or long-term in the sense of an „ensemble average" (ex. monthly averages averaged over many years). Such long-term averages show non-monotonic distributions of upwelling intensity as a function of latitude which seem to be typical for coastal upwelling areas characterized by upwelling maximums known as centers of upwelling. Fig. 1 (WOOSTER, 1970) shows for example a large center of upwelling at 14.5° S and weaker ones at 8° S and 30° S along the west coast of South America.

The causes for this long-term and for the fisheries certainly more important type of variability are not known with certainty. However, the following possible causes can be listed: 1. Topographical effects, 2. The effect of variable trade winds strength and persistency with latitude, 3. The interaction of the daily wind cycle (seabreeze-landbreeze) with the time-dependent velocity field (Fredholm's solution to the Ekman wind drift theory) (EKMAN, 1905).

The possible topographic effects that could lead to a local upwelling maximum are many. The first and most obvious effect is the orientation of the coastline relative to a "stationary" trade wind. For instance between 15° S and 19° S the western coast of South Africa is so orientated that the trade wind has an onshore component. This has a damping influence on the upwelling. Indeed fig. 1 indicates an upwelling minimum for these latitudes.

That a current flowing around a cape with a sufficiently small radius of curvature can result in upwelling downstream from the cape has been shown by ARTHUR (1965). With a typical horizontal velocity of 10 cm/s, a radius of curvature of about 50 km would be needed to produce a vertical velocity on the order of the steady-state vertical upwelling velocity. This effect could explain only small-scale (at most 1° in latitude) deviations in upwelling magnitude.

It is thought that the continental shelf, which is a prominent feature in all areas of coastal upwelling with the expection of the west coast of South America, plays an important role in upwelling. YOSHIDA (1967) as the first one to attack this problem found that the width of the continental shelf influences the width of the zone of upwelling and that the shallower the shelf, the more relatively intensive the vertical velocity at its outer edge.

It is clear that the trade wind variations with latitude will have an important effect on the magnitude of the resulting upwelling. This is most easily seen if one recalls the expression for the Ekman transport away from shore, τ/f (τ is the wind stress and f the Coriolis parameter). Most emperical wind stress relationships yield a dependence of the wind stress on the square of the wind velocity in the direction of the wind stress. Thus for example a coastal-parallel wind of 7 m/s would induce theoretically about twice as much upwelling as a wind of 5 m/s. In addition the persistency of the wind strength and direction could effect the upwelling intensity: Fredholm's solution shows that it takes about 1 or 2 days for the time-dependent velocity field to reach its steady state values (on a daily average) after the wind suddenly begins to blow. Then logically from continuity considerations the upwelling induced by a wind blowing parallel to the coast should be fully developed in about the same time scale. Thus the upwelling intensity would be expected to be greater at a latitude where the persistency

is high than at a latitude where the changeability inhibits tke full development of the upwelling field. However in practice the correlation between trade wind strength and persistency and upwelling intensity is hard to make. The lack of data from coastal upwelling areas is prohibitive.

By studying the wind field given for the north Atlantic in two-degree square units, (Markgraf 1955, 1960), I came however in a way similar to that of WOOSTER and REID (1963) to a coarse survey of how the upwelling intensity on the northwest coast of Africa should look based on the maps of wind strength and persistency. Upwelling should take place in some extent from 13° N to 31° N in winter and spring, in fall between 17° N and 31° and in summer between 20° N and 33° N. The upwelling is generally strongest in the winter and spring and weakest in the fall. Upwelling is strongest in the winter between 18° N and 23° N, in the spring between 18° N and 25° N, in the summer between 22° N and 28° N, and in the fall between 19° N and 23° N. This seems to correspond roughly to the admittedly sparce observations in this area (WOOSTER and REID, 1963). In any case a more exact knowledge of the wind conditions seem to be the key for explaining much of the spacial variation of upwelling intensity.

It is well known that a wind which suddenly begins to blow upon an ocean produces a time-dependent velocity field in the ocean which reaches a final, steady-state value after a certain length of time. This time-dependent velocity field oscillates with the inertial period (12 hours/sin Φ) about the final value. If a forcing function with a constant period (ex. the daily seabreeze-landbreeze cycle) is imposed upon this system, one would expect from wave theory a resonance point where the two periods are equal. This phenomenon and its possible consequences will be investigated in this paper.

2. Theoretical Treatment

2.1 The Problem is Posed

Consider a model ocean that is homogeneous, infinitely deep and infinitely wide. This ocean is bounded on one side by an infinitely long, straight coast in the form of a vertical wall extending in the north-south direction. At a time $t = 0$ a wind which varies in space and time begins to blow upon the ocean (the exact form of the wind to be used will be studied in detail later). This ocean as well as the coordinate system that will be used are shown in fig. 2. My positive x, y, and z coordinates are directed westward, southward, and downward respectively. For simplicity it is assumed that the wind does not vary in the y direction. It follows that the velocity field will be independent of y.

The simplified momentum equations for this system are:

$$(1) \quad \frac{\partial u}{\partial t} - fv = \nu_z \frac{\partial^2 u}{\partial z^2} + \nu_x \frac{\partial^2 u}{\partial x^2}$$

$$(2) \quad \frac{\partial v}{\partial t} + fu = \nu_z \frac{\partial^2 v}{\partial z^2} + \nu_x \frac{\partial^2 v}{\partial x^2}$$

whereby u, v are the velocities in the positive x, y directions respectively, f is the Coriolis parameter, and ν_z, ν_x are (assumed) constant vertical and horizontal eddy viscosities respectively.

The advective terms of form $u \cdot \Delta u$ are neglected because we are dealing with the eastern side of an ocean where currents are relatively broad and slow. The pressure gradient terms of the form $\frac{1}{\rho} \Delta_H p$, and therefore the surface slope, are neglected because of the homogeneity and infinite depth of the ocean.

The effect of a rigid sea surface as considered here is that the water that is blown away from the coast is compensated entirely by upwelling. Thus the assumption of a rigid sea surface could affect the magnitude of the upwelling but probably not the general property distribution.

The vertical velocity w itself will be derived with the help of the continuity equation,

$$(3) \quad \frac{\partial u}{\partial x} + \frac{\partial w}{\partial z} = 0$$

after the momentum equations have been solved.

It is convenient to treat this problem as it stands in complex notation. With the definition, $W = u + iv$, equations (1) and (2) can be combined to the form,

$$(4) \quad \nu_z \frac{\partial^2 W}{\partial z^2} + \nu_x \frac{\partial^2 W}{\partial x^2} - \frac{\partial W}{\partial t} - ifW = 0$$

The initial condition and boundary conditions needed to solve this equation are chosen to be,

$$(5) \quad W(x, z, o) = 0$$

$$(6) \quad W(o, z, t) = 0$$

$$(7) \quad W(\infty, z, t) = 0$$

$$(8) \quad \left.\frac{\partial W}{\partial x}\right|_{x=\infty} = 0$$

$$(9) \quad W(x, \infty, t) = 0$$

$$(10) \quad -\rho \nu_z \left.\frac{\partial W}{\partial z}\right|_{z=0} = \tau$$

where ρ is the density of the sea water taken as 1 g/cm^3, and τ is the complex wind stress.

The calculations to be made can now be simplified if we formally introduce non-dimensional variables. For this analysis it is practical to introduce these variables in the following form:

$$\overset{o}{x} \equiv \frac{\pi}{2} \frac{x}{D_x} ,$$

$$\overset{o}{z} \equiv \frac{\pi}{2} \frac{z}{D_z} ,$$

$$\overset{o}{t} \equiv ft ,$$

where $D_x \equiv \pi / \sqrt{f/\nu_x}$, $D_z \equiv \pi / \sqrt{f/\nu_z}$

are the width and depth of the coastal and surface Ekman layers respectively and correspond to the definitions given by Ekman (1905).

In terms of these new variables, eq. 4 becomes:

$$(11) \quad \frac{\partial^2 W}{\partial \overset{o}{z}^2} + \frac{\partial^2 W}{\partial \overset{o}{x}^2} - 4 \frac{\partial W}{\partial \overset{o}{t}} - 4 i W = 0$$

Tafel 1 (zu G. R. Shaffer)

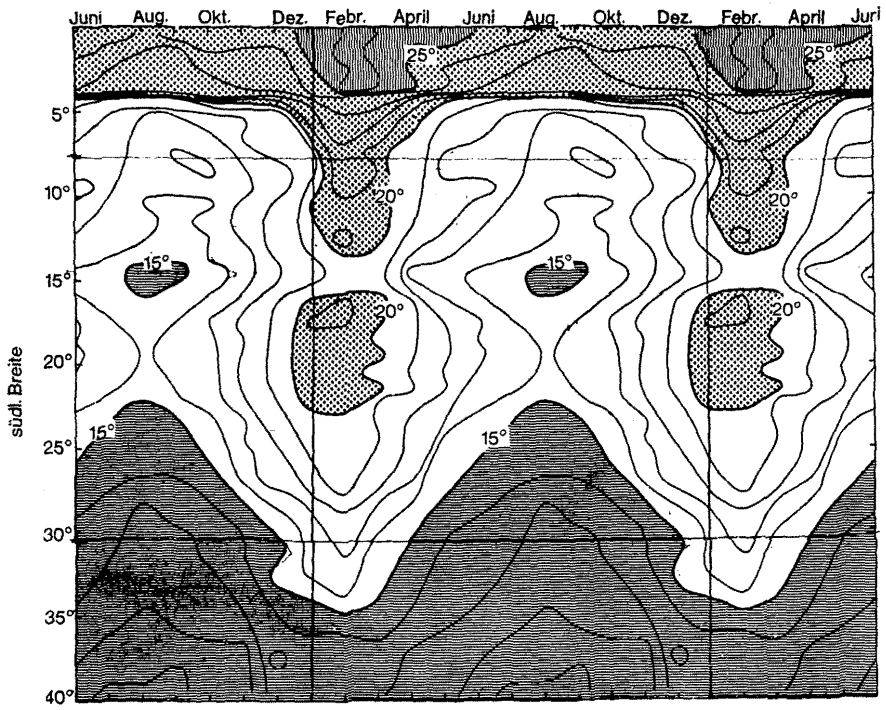

Fig. 1 Monthly surface temperature averages for 1-degree squares along the west coast of South America (Wooster, 1970).

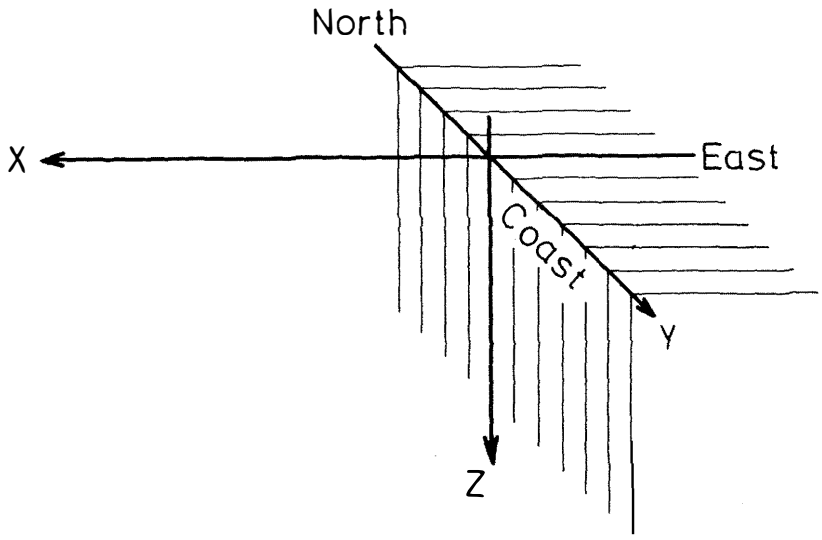

Fig. 2 The model ocean considered, showing the orientation of the coordinate axes.

Tafel 2 (zu G. R. Shaffer)

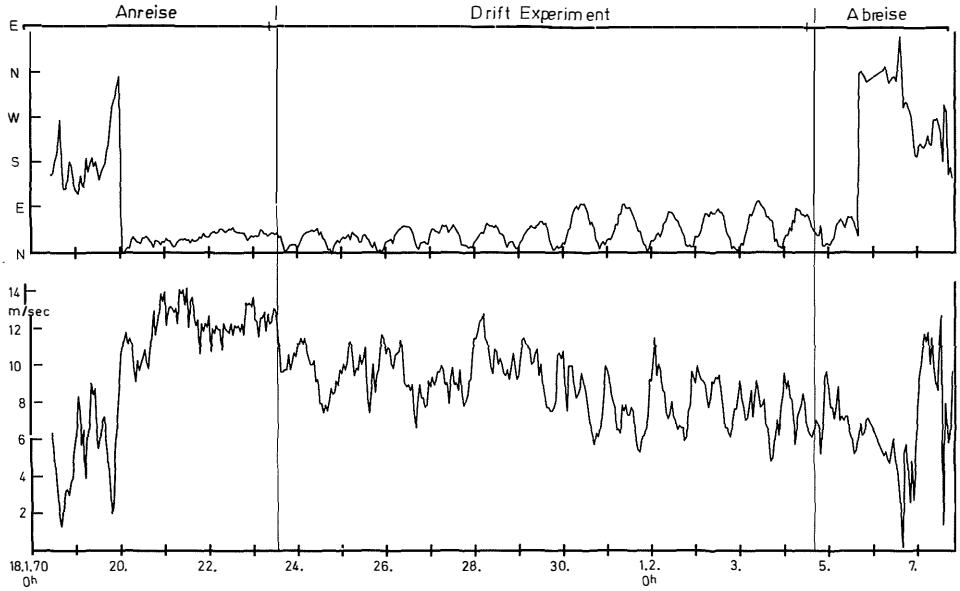

Fig. 3 The wind direction (above) and wind speed (below) of the wind measured during Jan. to Feb. 1970 as a part of the drift experiment aboard the "Meteor" by about 20° N and 120 km from the coast of north west Africa (Tomczak, 1973).

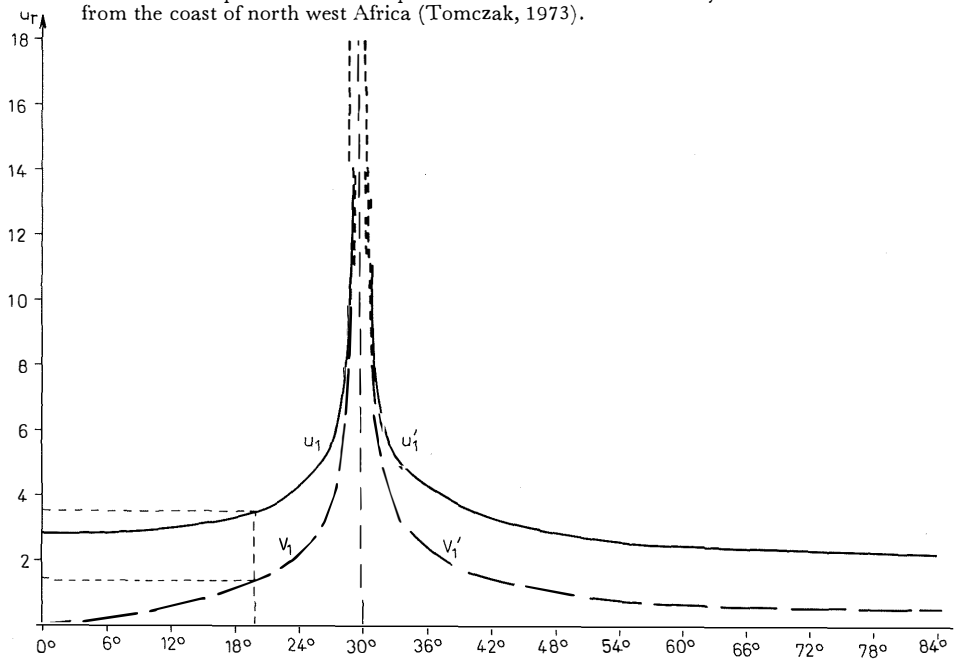

Fig. 4 The components of the periodic velocity field derived at the surface just outside the coastal Ekman layer in terms of u_r, a reference velocity, as a function of latitude. From our assumptions, u_r is found to be 3.4 cm/sec. Full line: east-west component (southeast-northwest component for u'_1). Broken line: north-south component (northeast-southwest component for v'_1).

The initial and boundary conditions with the exception of the last one are the same as the ones listed above (5—9) with the dimensional variables replaced by their corresponding non-dimensional variables. The last boundary condition (10) becomes:

$$(12) \qquad -\frac{\pi \rho \nu_z}{2 D_z} \frac{\partial W}{\partial z}\Bigg|_{z=0} = \tau(x, t)$$

2.2. The Wind Stress is Chosen

The choice of the wind stress model will determine the velocity distribution to a large degree, as one would expect since the wind stress is the only force working in the problem. HIDAKA (1954) and SAITO (1956), whose basic model oceans were quite similar to mine, used a wind stress that was constant in a certain wind belt (about twice the width of the coastal Ekman layer) and zero outside of it. This is hardly realistic. In the first place, the trade winds do not abruptly die out at a certain distance from the shore. Secondly their width is certainly greater than the assumed 200—300 km.

This wind stress model induces very strong convergence (sinking) at the outer edge of the wind belt which does not correspond to observations. With the real wind field, this convergence is gradual and the main driving force for the upwelling is the divergence caused by the wind blowing at the coast.

In an attempt to include as much realism as possible in my model without making it mathematically untractable, as well as to relate it to the upwelling off the northwest coast of Africa, I used the wind measurements given in fig. 3 (TOMCZAK, 1973) as a basis for a wind stress model. They were made on the "Meteor" expedition to northwest Africa in Jan.—Febr. 1970 at a distance of about 120 km from the coast and at 20° N latitude.

These measurements can be interpreted as follows: From Jan. 24 to Jan. 29, the strength of the northeast trade wind was about 8 m/s, from Jan. 30 to Febr. 5 about 6 m/s. In each case a time-variable wind with a period of one day and amplitude of 6 m/s is superimposed upon the trade wind and blows almost perpendicular to it. This is the seabreeze-landbreeze phenomenon with which most coastal dwellers are familiar. It is especially strong and well-developed in areas of coastal upwelling: upwelling coasts are deserts at low latitudes and thus receive very constant daily radiation warming. In addition the colder upwelled water off the coast cools the air above it increasing the temperature difference between the air above the land and the air above the water in the daytime. This should increase the amplitude of the wind.

In an effort to model the wind measurements in a way which retains their basic substance but allows a relatively simple expression for the wind stress, I arrived at the following expression:

$$(13) \qquad \tau = \tau_x \sin \omega t \exp(-\lambda_1 x) + i\tau_y \exp(-\lambda_2 x)$$

where τ_x, τ_y are the magnitudes of the wind stress by $x = 0$ in the x, y directions respectively, $\omega = 2\pi/24$ hours and λ_1, λ_2 are characteristic wave numbers which correspond to the inverse width of the landbreeze-seabreeze belt and the trade wind belt respectively.

In this expression, I have rotated the axis of the real coordinate system on the northwest coast of Africa by about 45° to obtain a trade wind which blows out of the sorth still parallel to the coast (the second term in (13)), and a seabreeze-landbreeze which blows in the east-west direction normal to the coast (the first term in (13)). This is just a formal step to simplify the problem and does not alter the physical situation (the more so since we are looking at local effects for which f is considered a constant).

In terms of our non-dimensional variables eq. (13) becomes:

$$\tau = \tau_x \sin \omega/f \overset{\circ}{t} \exp\left(-2 \overset{\circ}{\lambda}_1 \overset{\circ}{x}\right) + i\tau_y \exp\left(-2 \overset{\circ}{\lambda}_2 \overset{\circ}{x}\right) \tag{14}$$

where

$$\overset{\circ}{\lambda}_{1,2} \equiv \frac{D_x}{\pi} \lambda_{1,2} \ .$$

2.3. The Problem is Solved

The task before us now is to solve the second-order, homogeneous differential equation (11) for the given boundary conditions. This is most straightforwardly done by the methods of integral transformations.

First of all, a Fourier sine transformation is performed with respect to $\overset{\circ}{x}$. Given the definition,

$$V = \int_0^\infty W \sin \alpha \overset{\circ}{x}$$

and the non-dimensionalized boundary conditions, (6), (7) and (8), (11) becomes:

$$\frac{\partial^2 V}{\partial \overset{\circ}{z}^2} - 4 \frac{\partial V}{\partial \overset{\circ}{t}} - \left\{ \alpha^2 + 4\,i \right\} V = 0 \ . \tag{15}$$

The wind stress representation must also be transformed. With

$$\tilde{\tau} \equiv \int_0^\infty \tau \sin \alpha \overset{\circ}{x}\, d\overset{\circ}{x} \ ,$$

(14) becomes:

$$\tilde{\tau} = \tau_x \sin \omega/f \overset{\circ}{t} \left[\frac{\alpha}{\alpha^2 + 4 \overset{\circ}{\lambda}^2_1} \right] + i\,\tau_y \left[\frac{\alpha}{\alpha^2 + 4 \overset{\circ}{\lambda}^2_2} \right] \tag{16}$$

Thus the initial and the remaining boundary conditions are,

$$V(\alpha, \overset{\circ}{z}, 0) = 0 \tag{17}$$

$$V(\alpha, \infty, \overset{\circ}{t}) = 0 \tag{18}$$

$$-\frac{\pi \rho \nu_z}{2 D_z} \frac{\partial V}{\partial \overset{\circ}{z}} \Bigg|_{\overset{\circ}{z} = 0} \equiv \tau \tag{19}$$

The next step is to perform a Laplace transformation with respect to $\overset{\circ}{t}$ on (15). With

$$U \equiv \int_0^\infty e^{-s \overset{\circ}{t}} V\, d\overset{\circ}{t} \ ,$$

and the initial condition we have

$$\frac{\partial^2 U}{\partial \overset{\circ}{z}^2} - \{ \alpha + 4\,i + 4\,s \} U = 0 \tag{20}$$

The two remaining boundary conditions are,

(21) $U(\alpha, \infty, s) = 0$

(22) $$-\frac{\pi \rho \nu_z}{2 D_z} \frac{\partial U}{\partial \overset{\circ}{z}}\Bigg|_{\substack{\circ \\ z=0}} = \overset{\approx}{\tau}$$

where

$$\overset{\approx}{\tau} \equiv \int_0^\infty e^{-s \overset{\circ}{t}} \overset{\sim}{\tau} d \overset{\circ}{t}$$

The general solution to (20) can be given immediately. It is,

(23) $$U(\alpha, \overset{\circ}{z}, s) = c_1 \exp\left(-\sqrt{\alpha + 4_1 + 4s}\ \overset{\circ}{z}\right) + c_2 \exp\left(-\sqrt{\alpha + 4_1 + 4s}\ \overset{\circ}{z}\right)$$

Because of (21), $c_1 = 0$.

Then by differentiating the remaining term in (23) and applying the boundary condition (22) given above, we have,

(24) $$c_2 = \frac{2 D_z}{\pi \rho \nu_z \sqrt{\alpha + 4 i + 4 s}} \overset{\approx}{\tau} .$$

Therefore the final solution to (20) is,

(25) $$U(\alpha, \overset{\circ}{z}, s) = \frac{D_z \overset{\approx}{\tau}}{\pi \rho \nu_z \sqrt{\alpha^2/_4 + i + s}} \exp\left(-2\sqrt{\alpha^2/_4 + i + s}\ \overset{\circ}{z}\right)$$

Our task now is to transform the solution (25) back into the original, physical coordinates. Only then we can recognize the physical significance of it.

As the first step, I will perform an inverse Laplace transformation on (25). With help of the expression

$$L^{-1}\left(\frac{\exp(-a\sqrt{s})}{\sqrt{s}}\right) = \frac{\exp(-a^2/4\,\overset{\circ}{t})}{\sqrt{\pi\,\overset{\circ}{t}}}$$

and the translation property for Laplace transformations, one obtains,

(26) $$V(\alpha, \overset{\circ}{z}, \overset{\circ}{t}) = \frac{D_z}{\pi^{3}/_{2}\,\rho\,\nu_z} \int_0^{\overset{\circ}{t}} \overset{\sim}{\tau}(\alpha, \overset{\circ}{t} - \sigma) \frac{\exp\left(-\left(\frac{\alpha^2}{4} + i\right)\sigma - \frac{\overset{\circ}{z}^2}{\sigma}\right)}{\sqrt{\sigma}} d\sigma$$

This expression is in the form of a convolution integral.

Now by writing out the explicit form for the wind stress, grouping all the terms which contain α together, and with the help of the inverse Fourier sine Transformation:

$$F_{(s)}^{-1}\left(\frac{x}{b^2 + x^2} \exp(-a^2 x^2)\right) = \frac{1}{2} e^{a^2 b^2} \cdot$$

$$\cdot \left[\exp(-by)\,\Phi\left(ab - \frac{y}{2a}\right) - \exp(by)\,\Phi\left(ab + \frac{y}{2a}\right)\right]$$

where

$$\Phi(x) \equiv \operatorname{Erfc}(x) \equiv \frac{2}{\sqrt{\pi}} \int_x^\infty \exp(-t^2)\, dt$$

one can finally write an expression for the velocity field in the original coordinates in a form which gives the time development of the velocity field. Thus we have,

$$(27)\quad W = \frac{D_z}{2\pi^{3/2}\rho\nu_z} \int_0^{\overset{\circ}{t}} \frac{\exp\left(-i\sigma - \frac{\overset{\circ}{z}^2}{\sigma}\right)}{\sqrt{\sigma}} \left\{ \tau_x \sin\frac{\omega}{f}(\overset{\circ}{t}-\sigma) \right.$$

$$\exp(\overset{\circ}{\lambda}_1{}^2\sigma)\left[\exp(-2\overset{\circ}{\lambda}_1\overset{\circ}{x})\,\Phi\left(\overset{\circ}{\lambda}_1\sqrt{\sigma} - \frac{\overset{\circ}{x}}{\sqrt{\sigma}}\right) - \right.$$

$$\left.\left. \exp(2\overset{\circ}{\lambda}_1\overset{\circ}{x})\,\Phi\left(\overset{\circ}{\lambda}_1\sqrt{\sigma} + \frac{\overset{\circ}{x}}{\sqrt{\sigma}}\right)\right] + i\tau_y \exp(\overset{\circ}{\lambda}{}^2_2\sigma) \right.$$

$$\left. \left[\exp(-2\overset{\circ}{\lambda}_2\overset{\circ}{x})\,\Phi\left(\overset{\circ}{\lambda}_2\sqrt{\sigma} - \frac{\overset{\circ}{x}}{\sqrt{\sigma}}\right) - \exp(2\overset{\circ}{\lambda}_2\overset{\circ}{x})\,\Phi\left(\overset{\circ}{\lambda}_2\sqrt{\sigma} + \frac{\overset{\circ}{x}}{\sqrt{\sigma}}\right)\right] \right\} d\sigma$$

where σ is the integration variable.

After making use of the trigonometric identity

$$\sin\frac{\omega}{f}(\overset{\circ}{t}-\sigma) = \sin\frac{\omega}{f}\overset{\circ}{t}\cos\frac{\omega}{f}\sigma - \cos\frac{\omega}{f}\overset{\circ}{t}\sin\frac{\omega}{f}\sigma\ ,$$

various trigonometric identities for the multiplication of two sinusoidal functions, and dividing (27) into the real and imaginary parts, we can write,

$$(28)\quad u = \frac{D_z\,\tau_x}{4\,\pi^{3/2}\rho\,\nu_z} \left\{ \sin\frac{\omega}{f}\overset{\circ}{t} \int_0^{\overset{\circ}{t}} \left[\cos\left(\frac{\omega}{f}+1\right)\sigma + \cos\left(\frac{\omega}{f}-1\right)\sigma \right] \right.$$

$$\frac{\exp\left(\frac{-\overset{\circ}{z}^2}{\sigma}\right)}{\sqrt{\sigma}}\ \textcircled{H}\,\overset{\circ}{\lambda}_1\, d\sigma - \cos\frac{\omega}{f}\overset{\circ}{t} \int_0^{\overset{\circ}{t}} \left[\sin\left(\frac{\omega}{f}+1\right)\sigma + \sin\left(\frac{\omega}{f}-1\right)\sigma \right] \cdot$$

$$\frac{\exp\left(\frac{-\overset{\circ}{z}^2}{\sigma}\right)}{\sqrt{\sigma}}\ \textcircled{H}\,\overset{\circ}{\lambda}_1\, d\sigma + \frac{D_z\,\tau_y}{2\,\pi^{3/2}\rho\,\nu_z} \int_0^{\overset{\circ}{t}} \sin\sigma\ \frac{\exp\left(\frac{-z^2}{\sigma}\right)}{\sqrt{\sigma}}\ \textcircled{H}\,\overset{\circ}{\lambda}_2\, d\sigma\ ,$$

$$(29)\quad v = \frac{D_z\,\tau_x}{4\,\pi^{3/2}\rho\,\nu_z} \left\{ \sin\frac{\omega}{f}\overset{\circ}{t} \int_0^{\overset{\circ}{t}} \left[\sin\left(\frac{\omega}{f}-1\right)\sigma - \sin\left(\frac{\omega}{f}+1\right)\sigma \right] \right.$$

$$\frac{\exp\left(\frac{-\overset{\circ}{z}^2}{\sigma}\right)}{\sqrt{\sigma}}\ \overset{\circ}{\underset{\lambda_1}{\text{Ⓗ}}}\ d\sigma + \cos\frac{\omega}{f}\overset{\circ}{t}\int_0^{\overset{\circ}{t}}\left[\cos\left(\frac{\omega}{f}-1\right)\sigma - \cos\left(\frac{\omega}{f}+1\right)\sigma\right].$$

$$\frac{\exp\left(\frac{-\overset{\circ}{z}^2}{\sigma}\right)}{\sqrt{\sigma}}\ \overset{\circ}{\underset{\lambda_1}{\text{Ⓗ}}}\ d\sigma + \frac{D_z\,\tau_x}{2\,\pi^{3}/_{2}\,\rho\,\nu_z}\int_0^{\overset{\circ}{t}}\cos\sigma\ \frac{\exp\left(\frac{-z^2}{\sigma}\right)}{\sqrt{\sigma}}\ \overset{\circ}{\underset{\lambda_2}{\text{Ⓗ}}}\ d\sigma\ .$$

where

$$\overset{\circ}{\underset{\lambda_j}{\text{Ⓗ}}} = \exp(\overset{\circ}{\lambda_j}^2\sigma)\left[\exp(-2\,\overset{\circ}{\lambda_j}\,\overset{\circ}{x})\cdot\Phi\left(\overset{\circ}{\lambda_j}\sqrt{\sigma} - \frac{\overset{\circ}{x}}{\sqrt{\sigma}}\right) - \exp(2\,\overset{\circ}{\lambda_j}\,\overset{\circ}{x})\cdot\Phi\left(\overset{\circ}{\lambda_j}\sqrt{\sigma} + \frac{\overset{\circ}{x}}{\sqrt{\sigma}}\right)\right]$$

In order to obtain the equation for the vertical velocity field, which of course is of the most immediate interest in a theoretical study concerning upwelling, we use the continuity equation in our dimensionless variables to get

$$(30)\qquad w(\overset{\circ}{x},\overset{\circ}{z},\overset{\circ}{t}) = -\frac{D_z}{D_x}\int_0^{\overset{\circ}{z}}\frac{\partial u}{\partial\overset{\circ}{x}}\,dz'$$

whereby it is assumed that

$$(31)\qquad w(\overset{\circ}{x},o,\overset{\circ}{t}) = 0$$

After differentiation of (28) by $\overset{\circ}{x}$ and integration over $\overset{\circ}{z}$ we arrive at this expression for w:

$$(32)\qquad w = -\frac{D^2{}_z\,\tau_x}{4\,\pi^{3}/_{2}\rho\,\nu_z D_x}\left\{\sin\frac{\omega}{f}\overset{\circ}{t}\cdot\right.$$

$$\cdot\int_0^{\overset{\circ}{t}}\frac{\left[\cos\left(\frac{\omega}{f}+1\right)\sigma+\cos\left(\frac{\omega}{f}-1\right)\sigma\right]}{\sqrt{\sigma}}\ \frac{\partial\,\overset{\circ}{\underset{\lambda_1}{\text{Ⓗ}}}}{\partial\overset{\circ}{x}}\left(\int_0^{\overset{\circ}{z}}\exp\left(\frac{-\overset{\circ}{z}^2}{\sigma}\right)dz'\right)\ d\sigma$$

$$\left.-\cos\frac{\omega}{f}\overset{\circ}{t}\int_0^{\overset{\circ}{t}}\frac{\left[\sin\left(\frac{\omega}{f}+1\right)\sigma+\sin\left(\frac{\omega}{f}-1\right)\sigma\right]}{\sqrt{\sigma}}\ \frac{\partial\,\overset{\circ}{\underset{\lambda_1}{\text{Ⓗ}}}}{\partial x}\left(\int_0^{\overset{\circ}{z}}\exp\left(\frac{-\overset{\circ}{z}^2}{\sigma}\right)dz'\right)d\sigma\right\}$$

$$+\frac{D_z^2\,\tau_y}{2\,\pi^{3}/_{2}\,\rho\,\nu_z D_x}\int_0^{\overset{\circ}{t}}\frac{\sin\sigma}{\sqrt{\sigma}}\ \frac{\partial\,\overset{\circ}{\underset{\lambda_2}{\text{Ⓗ}}}}{\partial\overset{\circ}{x}}\left(\int_0^{\overset{\circ}{z}}\exp\left(\frac{-\overset{\circ}{z}^2}{\sigma}\right)dz'\right)d\sigma$$

where

$$(33)\qquad \frac{\partial \overset{\circ}{\Theta}_{\lambda_j}}{\partial \overset{\circ}{x}} = \left\{ \frac{4}{\sqrt{\pi\sigma}} \exp\left(-\frac{\overset{\circ}{x}^2}{\sigma}\right)\right\}$$

$$-\left\{ 2\,\overset{\circ}{\lambda}_j \exp(\overset{\circ}{\lambda}{}^2_j\,\sigma)\left[\exp(-2\,\overset{\circ}{\lambda}_j\,\overset{\circ}{x}) \cdot \Phi\left(\overset{\circ}{\lambda}_j\sqrt{\sigma} - \frac{\overset{\circ}{x}}{\sqrt{\sigma}}\right) + \exp(2\,\overset{\circ}{\lambda}_j\,\overset{\circ}{x}) \cdot \right.\right.$$

$$\left.\left. \cdot \Phi\left(\overset{\circ}{\lambda}_j\sqrt{\sigma} + \frac{\overset{\circ}{x}}{\sqrt{\sigma}}\right)\right]\right\}$$

$$= \{a\} - \{b\}\,.$$

3. A Discussion

3.1. The Complete Equations are Studied

Equations (28), (29) and (32) which describe the velocity field as a function of space and time are in their complete form too complicated to visualize the exact distribution of the velocity field. Nevertheless, certain details about it can be given.

Each velocity component contains two harmonic terms which oscillate with the period of one day and whose amplitudes are given by time integrals. These terms describe the response of the system to the periodic seabreeze-landbreeze wind stress which suddenly begins to blow. The third term of each velocity component describes the response of the system to the trade wind that suddenly begins to blow. It is similiar to the solutions obtained by Saito, but differs of course in the x-variation, a result of the different assumptions concerning the form of the wind stress. This term is essentially a Fredholm solution with the addition of a variation in the x-direction which results first of all from the presence of a boundary and secondly from the x-variation of the wind stress model.

The amplitudes of the harmonic terms have been brought into a form which is similiar to the Fredholm solution (with an x-variation), differing only in the argument of the sin and cos within the integrals. It is assumed that the time integrals converge to consistant values for every point in the ocean after a certain length of time. The spacial variation contained under the integrals as well as the values for the $\overset{\circ}{\lambda}$'s will in general mean that this "convergence time" will also be a function of space and the $\overset{\circ}{\lambda}$'s. Indeed one might speculate that the time required for convergence could at certain points be so large that a constant, non-oscillating condition might never be reached in the real world. (Fig. 3 is an illustration of the fact that in the real world the trade winds and the seabreeze-landbreeze do indeed change with time in a non-periodic manner. Each such change might be considered in some way equivalent to a wind that suddenly begins to blow).

The vertical variation of the horizontal velocities is the same as that of Fredholm's solution. Accordingly one will expect to find no significant horizontal velocity below the bottom of the Ekman layer.

The vertical velocity is of course of special interest to us. The x-variation of w which is given in eq. 33, suggests that the vertical velocity consists of two parts. The first part called (a) is directed in the negative z direction, that is upwardly directed. This represents the upwelling itself caused by the trade winds in a narrow coastal zone (I am here refering to the third term in eq. (32).) The form of (a) is identical with the z-variation of the horizontal velocities with z replaced by x. Thus by analogy this describes the

vertical velocity distribution within the coastal Ekman layer and indicates that there will be no effective upwelling outside of it. This in turn shows that the width of the zone of coastal upwelling is about D_x. The magnitude of D_x will be estimated later. Furthermore this means that theoretically the width of the upwelling zone should grow as one approaches the equator by the definition of D_x. This seems to agree with observations for the coast of Peru and Chile (WYRTKI, 1964).

The term (b) represents the second part of the vertical velocity. It describes a downward motion and results from the convergence of the wind field model. If $\overset{\circ}{\lambda}_2$ were zero, the wind field would be constant and would induce no convergence in the ocean. If $\overset{\circ}{\lambda}_2$ were of order 1, one would expect to have a downward motion in the coastal Ekman layer of the same order of magnitude as the upwelling, in effect reducing it. In reality $\overset{\circ}{\lambda}_2$ lies between 0 and 1.

For the harmonic terms of the vertical velocity field, (a) and (b) describe two wave-like motions, 180° out of phase with each other within the coastal Ekman layer and within the landbreeze-seabreeze belt respectively.

The z-variation of w indicates that w remains essentially constant and maximum from the bottom of the Ekman layer downwards.

3.2. Simplifications are Made

3.2.1. Fredholm's Solution

In order to check the results obtained in section 2 as well as to bring the answers obtained into a form which allows a more detailed, if somewhat idealized, discussion of them, it is useful to make certain simplifications. In general this means that we will consider the equations (28), (29) and (32) for extreme values of the variables and parameters.

We will begin by discussing the third term of equations (28), (29) and (32). This is the term, as we recall, that results from the trade wind that suddenly begins to blow. First of all we will investigate the behavior of the equations for $\overset{\circ}{\lambda}_2 \to 0$, i.e. for a constant wind blowing over the entire ocean. This in effect eliminates one source of the x-variation in the velocity field. Then, for instance, the third component of eq. 28, u_3, becomes,

$$(34)\quad u_3 = \frac{D_z D_y}{2\pi^{3/2}\rho\nu_z}\int_0^{\overset{\circ}{t}} \sin\sigma \exp\left(-\frac{\overset{\circ}{z}^2}{\sigma}\right)\frac{\left[\Phi\left(-\frac{\overset{\circ}{x}}{\sqrt{\sigma}}\right)-\Phi\left(\frac{\overset{\circ}{x}}{\sqrt{\sigma}}\right)\right]}{\sqrt{\sigma}}\,d\sigma$$

As the next step we consider eq. (34) for a large $\overset{\circ}{x}$. This means that we go far enough away from the coast. to be able to neglect its effect. Since we have already seen that the effect of the coast is practically restricted to the coastal zone of order D_X, this condition should be approximately met outside the coastal Ekman layer. Thus we eliminate the second source of the x-variation of the velocity field and would expect to obtain the solution of the equation pair (1) and (2) minus the last term in each of form:

$$\nu_x \frac{\partial^2 u}{\partial x^2}\quad,\quad \nu_x \frac{\partial^2 v}{\partial x^2}$$

But this solution for a constant wind stress is already known. It is Fredholm's solution to the Ekman problem. With that we have the first chance to check the solution given

in section 2. Since

$$\Phi(x) = \frac{2}{\sqrt{\pi}} \int_{x}^{\infty} \exp(-x'^2)\, dx ,$$

and since $\exp(-x^2)$ is an even function, the term

$$\left[\Phi\left(\frac{-\overset{\circ}{x}}{\sqrt{\sigma}}\right) - \Phi\left(\frac{\overset{\circ}{x}}{\sqrt{\sigma}}\right) \right] \underset{\overset{\circ}{x} > 1}{\Longrightarrow} \frac{2}{\sqrt{\pi}} \left[\sqrt{\pi} - 0\right] = 2$$

whereby $\sqrt{\sigma}$ is considered small with respect to $\overset{\circ}{x}$. Then (34) becomes,

$$(35) \quad u_3(\overset{\circ}{z}, \overset{\circ}{t}) = \frac{D_z \tau_y}{\pi^{3/2} \rho \nu_z} \int_{0}^{\overset{\circ}{t}} \sin\sigma \, \frac{\exp\left(\frac{-\overset{\circ}{z}^2}{\sigma}\right)}{\sqrt{\sigma}} \, d\sigma .$$

This is Fredholm's solution in the non-dimensional variables. Exactly the same procedure can be carried out for the north-south velocity component, v_3, and yields

$$(36) \quad v_3(\overset{\circ}{z}, \overset{\circ}{t}) = \frac{D_z \tau_y}{\pi^{3/2} \rho \nu_z} \int_{\overset{\circ}{0}}^{\overset{\circ}{t}} \cos\sigma \, \frac{\exp\left(\frac{-\overset{\circ}{z}^2}{\sigma}\right)}{\sqrt{\sigma}} \, d\sigma .$$

3.2.2. The Periodic Terms

The first two terms of equations (28), (29) and (32) can be evaluated in a similiar way as in the last sub-section. These are the terms which result from a daily seabreeze-landbreeze which suddenly begins to blow. Again an investigation of the behavior of the equations for $\overset{\circ}{\lambda}_1 = 0$ should prove fruitful. In this case however it is clear that in general the width of the coastal belt affected by this type of wind will be much less than the total width of the trade wind belt. It is therefore more difficult to justify taking $\overset{\circ}{\lambda}_1 = 0$. However if we again consider the area outside the coastal Ekman layer but still within the region effected by the seabreeze-landbreeze, we will approach a situation of minimal x-variation which is what we want.

Assuming this can be done, we can then write the first two terms of the east-west and north-south velocity components given in eqs. (28), (29), calling them u_1 and v_1 respectively, in analog to eq. (35) as follows:

$$(37) \quad u_1(\overset{\circ}{z}, \overset{\circ}{t}) = \frac{D_z \tau_x}{2\pi^{3/2} \rho \nu_z} \left\{ \sin\frac{\omega}{f}\overset{\circ}{t} \right.$$

$$\left. \int_{0}^{\overset{\circ}{t}} \left[\cos\left(\frac{\omega}{f} + 1\right)\sigma + \cos\left(\frac{\omega}{f} - 1\right)\sigma \right] \frac{\exp\left(\frac{-\overset{\circ}{z}^2}{\sigma}\right)}{\sqrt{\sigma}} \, d\sigma \right.$$

$$- \cos \frac{\omega}{f} \overset{\circ}{t} \int_0^{\overset{\circ}{t}} \left[\sin \left(\frac{\omega}{f} + 1 \right) \sigma + \sin \left(\frac{\omega}{f} - 1 \right) \sigma \right] \frac{\exp \left(\frac{- \overset{\circ}{z}^2}{\sigma} \right)}{\sqrt{\sigma}} \, d\sigma \Bigg\}$$

and

$$(38)\quad v_1 (\overset{\circ}{z}, \overset{\circ}{t}) = \frac{D_z \tau_x}{2 \pi^{3/2} \rho \nu_z} \Bigg\{ \sin \frac{\omega}{f} \overset{\circ}{t} \cdot$$

$$\int_0^{\overset{\circ}{t}} \left[\sin \left(\frac{\omega}{f} - 1 \right) \sigma - \sin \left(\frac{\omega}{f} + 1 \right) \sigma \right] \frac{\exp \left(\frac{- \overset{\circ}{z}^2}{\sigma} \right)}{\sqrt{\sigma}} \, d\sigma$$

$$+ \cos \frac{\omega}{f} \overset{\circ}{t} \int_0^{\overset{\circ}{t}} \left[\cos \left(\frac{\omega}{f} - 1 \right) \sigma - \cos \left(\frac{\omega}{f} + 1 \right) \sigma \right] \frac{\exp \left(\frac{- \overset{\circ}{z}^2}{\sigma} \right)}{\sqrt{\sigma}} \, d\sigma \Bigg\}$$

for "large" $\overset{\circ}{x}$.

We now let $\overset{\circ}{t} \to \infty$, where we assume that the above form holds in this limit and look at the solutions at $\overset{\circ}{z} = 0$ for simplicity. The integrals take on the form

$$\int_0^{\infty} \frac{\sin (a \pm 1)}{\sqrt{x'}} \, x' \, dx', \int_0^{\infty} \frac{\cos (a \pm 1)}{\sqrt{x'}} \, x' \, dx' .$$

From tables of definite integrals we have

$$\int_0^{\infty} \frac{\sin bx}{\sqrt{x}} \, dx = \int_0^{\infty} \frac{\cos bx}{\sqrt{x}} \, dx = \sqrt{\frac{\pi}{2 b}} \, , \; b > 0.$$

The conditions that $b > 0$, means that $a > 1$ for the equations above to be true. In other words we have with $a \equiv \frac{\omega}{f}$ the condition,

$$\frac{\omega}{f} = \frac{1}{2 \sin \varphi} > 1$$

where φ is the latitude or $\omega > f$. This is true when $\sin \varphi < 1/2$ or below 30° N latitude (we are considering in particular, the north-west coast of Africa). Then equations (37), (38) become

$$(39)\quad u (\overset{\circ}{z} = 0, \overset{\circ}{t} \gg 1) = \frac{D_z \tau_x}{2 \sqrt{2 \pi \rho \nu_z}} \left[\frac{(a + 1)^{1/2} + (a - 1)^{1/2}}{(a^2 - 1)^{1/2}} \right] \cdot$$

$$[\sin a \overset{\circ}{t} - \cos a \overset{\circ}{t}] ,$$

$$(40)\quad v_1\,(\overset{\circ}{z}=0,\ \overset{\circ}{t}\gg 1)=\frac{D_z\,\tau_x}{2\sqrt{2}\,\pi\,\rho\,\nu_z}\left[\frac{(a+1)^{1/2}-(a-1)^{1/2}}{(a^2-1)^{1/2}}\right]\cdot$$

$$\cdot\,[\sin a\overset{\circ}{t}+\cos a\overset{\circ}{t}]\,.$$

Equations (39), (40) describe a clockwise, elliptical, wave-like motion, whose major axis runs east and west and whose minor axis runs north and south. The amplitude of both the u- and v-component vary with the latitude in such a way that the mode of motion approaches a circle of large amplitude as φ approaches 30° and a pure, east-west oscillation of small amplitude as one approaches the equator. This is most easily seen if we write u_1 and v_1 in still another form which includes the complete variation with φ (a part of it was hidden in D_z).

$$41\quad u_1\,(\overset{\circ}{z}=0,\ \overset{\circ}{t}\gg 1)=\frac{\tau_x}{2\sqrt{2}\,\rho\,\nu_z^{1/2}}\left[\frac{(\omega+f)^{1/2}+(\omega-f)^{1/2}}{(\omega^2-f^2)^{1/2}}\right]\cdot$$

$$\cdot\left[\sin\left(\frac{\omega}{f}\overset{\circ}{t}-\frac{\pi}{4}\right)\right],$$

$$(42)\quad v_1\,(\overset{\circ}{z}=0,\ \overset{\circ}{t}\gg 1)=\frac{\tau_x}{2\sqrt{2}\,\rho\,\nu_z^{1/2}}\left[\frac{(\omega+f)^{1/2}-(\omega-f)^{1/2}}{(\omega^2-f^2)^{1/2}}\right]\cdot$$

$$\cdot\left[\sin\left(\frac{\omega}{f}\overset{\circ}{t}+\frac{\pi}{4}\right)\right].$$

From these equations one sees that as 30° N latitude is approached from the south, the amplitude of both components grows large since the denominator approaches zero. At 30° N the amplitude would become infinite mathematically and exhibit the character of a resonance point. The physical consequences of this behavior will be examined later.

A more detailed description of the variation of the amplitude of the u_1-wave is given in the lefthand side of fig. 4 in terms of a reference velocity u_r which will be determined later. It also gives, on the same side, the variation of the v_1-wave amplitude in terms of the same u_r.

In order to study this wave motion for latitudes above 30° N it is necessary to re-write equations (37) and (38) to satisfy the condition that $b > 0$. Above 30°, $f > \omega$; then the argument $\left(\frac{\omega}{f}-1\right)$ would be negative. Since sine is an odd function and cosine is an even function, it we substitute the argument $(1-\omega/f)$ for $(\omega/f-1)$, we obtain for (37) and (38) at $\overset{\circ}{z}=0$ and for $t\to\infty$)

$$(43)\quad u_1\,(\overset{\circ}{z}=0,\ \overset{\circ}{t}\gg 1)=\frac{D_z\,\tau_x}{2\sqrt{2}\,\pi\,\rho\,\nu_z}\left\{\left[\frac{(1+a)^{1/2}+(1-a)^{1/2}}{(1-a^2)^{1/2}}\right],\right.$$

$$\left.\cdot\,\sin a\overset{\circ}{t}+\left[\frac{(1+a)^{1/2}-(1-a)^{1/2}}{(1-a^2)^{1/2}}\right]\cos a\overset{\circ}{t}\right.,$$

and

$$(44)\quad v_1\,(\overset{\circ}{z}=0,\ \overset{\circ}{t}\gg 1)=\frac{D_z\,\tau_x}{2\sqrt{2}\,\pi\,\rho\,\nu_z}\left\{-\left[\frac{(1+a)^{1/2}+(1-a)^{1/2}}{(1-a)^{1/2}}\right]\right.\cdot$$

$$\cdot \sin a\,\overset{\circ}{t} + \left[\frac{(1+a)^{1/2} - (1-a)^{1/2}}{(1-a^2)^{1/2}} \right] \cos a\,\overset{\circ}{t} \quad .$$

These two equations again describe an ellipse. This time however the major axis is inclined 45° to the right of the positive x-direction. But in other respects it is similar to the results below 30° N. The movement is clockwise and the amplitudes of u_1 and v_1 vary in such a way that the mode of motion approaches a circle of large amplitude as φ approaches 30° but 0 for $f \to \infty$ (if it could: on the earth $f = 2\,\omega$ is the maximum value). This mode of motion is more easily seen if we define new velocities by vector addition,

$$\vec{u}' = \vec{u}_1 - \vec{v}_1,$$

and

$$\vec{v}' = \vec{u}_1 + \vec{v}_1 \quad .$$

Since the magnitudes of u_1, v_1 are equal, u' and v' describe the velocity field 45° to the left and to the right of u_1 respectively. The new expressions for the velocity field become:

$$(45) \quad u'\,(\overset{\circ}{z} = 0, \overset{\circ}{t} \gg 1) = \frac{\tau_x}{2\sqrt{2}\,\rho\,\nu_z^{1/2}} \left[\frac{(f+\omega)^{1/2} + (f-\omega)^{1/2}}{(f^2-\omega^2)^{1/2}} \right] \sin \frac{\omega}{f}\,\overset{\circ}{t} \quad ,$$

$$(46) \quad v'\,(\overset{\circ}{z} = 0, \overset{\circ}{t} \gg 1) = \frac{\tau_x}{2\sqrt{2}\,\rho\,\nu_z^{1/2}} \left[\frac{(f+\omega)^{1/2} - (f-\omega)^{1/2}}{(f^2-\omega^2)^{1/2}} \right] \cos \frac{\omega}{f}\,\overset{\circ}{t} \, .$$

The variations of u' and v' with latitude are given in the right side of fig. 4.

Fig. 4 represents a system with a forcing function with constant frequency (in our case the frequency of the seabreeze-landbreeze is always $2\,\pi/24$ hours), but a spacially-variable natural frequency (the inertial frequency). This is just the opposite of most systems which have a constant natural frequency and a forcing function of variable frequency. But the physical meaning is essentially the same.

At $f = 0$ on the equator one would expect the motion to have only an east-west component, because there is no diverting „force" to the right or to the left there.

The fact that above 30° the ellipses are inclined 45° to the right of the oscillating wind stress, also seems to have a simple physical explanation: By large f but before $f \to \infty$ the time that it takes for the system to reach the final steady state is proportional to $1/f$. By large enough f, this time scale will be small compared to 1 day. Thus the system will reach a steady state almost immediately: at the surface, 45° to the right of the applied wind stress. Thus an alternating wind stress like the one we have will induce an alternating current 45° to the right of it for large f as we can infer by comparing the curves of figure 4. Although in the real world we are of course restricted to $f \leqslant 2\,\omega$, the effect described above and the fact that f itself increases should help to explain the deviation of the major axis of the ellipses in the region $\omega \leqslant f \leqslant 2\,\omega$.

4. The Vertical Velocity: Numerical Examples

4.1 The Stationary Upwelling is Determined

Before proceeding directly to the determination of the upwelling, we must make educated guesses about the values of the parameters that until now have always been called constant or to be determined.

The values of υ_x, υ_z, the horizontal and vertical kinematic eddy viscosities, are usually considered to be between 10^7—10^9 and 10^1—10^3 respectively in cgs units. I have chosen to use the popular estimates, 10^8 and 10^2 respectively.

At 20° N which I have chosen as a typical upwelling latitude, f has the value

$$1.46 \sin 20° \times 10^{-4} = 5.0 \times 10^{-5}.$$

With these values we have

$$D_x = 45 \text{ km and } D_z = 45 \text{ m}$$

The magnitude of D_x corresponds well to the widths of the coastal upwelling zones often given of about 50 km (SMITH 1968).

Our main task now is to give the form of the wind stress explicitly whereby τ_x, τ_y, $\overset{\circ}{\lambda}_1$, and $\overset{\circ}{\lambda}_2$ must be determined. The wind charts of the north Atlantic show that the distance from the coast of Northwest Africa to the area of very light winds (the center of the Bermuda High) is about 2500 km. If we assume that the wind stress here is about $^1/_{10}$ of the wind stress at the coast, then we have $\overset{\circ}{\lambda}_2 = {}^1/_{1000}$ km and $\overset{\circ}{\lambda}_2 = 1.4 \times 10^{-2}$. For a wind velocity of 8 m/s at 120 km from shore as illustrated in fig. 3, τ_y would be 1.4 dynes/cm^2. In determining τ, the formula $\tau = 2.0 \times 10^{-3} \rho_{air} u_a^2$ is used where u_a is the measured wind velocity at anemometer height in cm/s. The constant 2.0×10^{-3} was chosen after some investigation of the various estimations of it. The often assumed value of 2.6×10^{-3} proves to be too large. There is certainly nothing holy about the choice of 2.0×10^{-3}, but the step of going from the wind speed to the wind stress is a notoriously weak point in any theory that has to use it.

The determination of $\overset{\circ}{\lambda}_1$ is harder since there are no wind charts for the variation of the magnitude of the seabreeze-landbreeze with distance from the coast. It seems logical to assume that the width and intensity of this daily wind cycle will depend on the area of land heated by the sun inland from the coast involved in this daily cycle. Thus, one would expect the seabreeze-landbreeze to be much better developed off the northwest coast of Africa than off the coast of Chile with its Andes for example. The 6 m/s velocity at 120 km from the coast as shown in fig. 3 seems to justify this. In addition since one would not expect extreme winds (over 10 m/s at the coast) from this daily cycle, one can assume that $\overset{\circ}{\lambda}_1$ is less than 1. I have chosen 500 km to be the distance at which $\tau = \frac{1}{10} \tau_x$, this means $\lambda_1 = 1/200$ km and $\overset{\circ}{\lambda}_1 = 7 \times 10^{-2}$. This implies that the amplitude of the seabreeze-landbreeze cycle at the coast is 8 m/s, a reasonable guess. Thus $\tau_x = 1.3$ dynes/cm^2. With the values of the parameters determined, we can deduce the order of magnitude of the various velocity components.

If we for example consider that the Ekman solution for the steady part of the velocity field is true at $x = D_x$, then we have that

$$u_3 (\overset{\circ}{z} = 0, \overset{\circ}{t} \to \infty) = \frac{1.30}{1.0 \sqrt{2 (5 \times 10^{-5}) (10^2)}} = 13 \text{ cm/sec} \quad .$$

The total Ekman transport away from the coast is

$$\frac{\tau_y}{f} = \frac{1.3}{5 \times 10^{-5}} = 2.6 \times 10^4 \text{ g/cm-sec} = \bar{\rho} \bar{u} D_z \Rightarrow \bar{u} = 6.0 \text{ cm/sec}$$

where $\bar{u}$ is considered to be a typical velocity in the surface Ekman layer, after the system has reached a steady state. But now we can say that all the water carried away westwards at $x = D_x$ must have been upwelled within the coastal Ekman layer. Then $\bar{u} D_z = \bar{w} D_x$, where $\bar{w}$ is a typical upward velocity within the coastal Ekman layer. This implies that $\bar{w} = 6.0 \times 10^{-3}$ cm/sec or 150 meter/month, somewhat greater than most estimates of coastal upwelling (SMITH, 1968). But we can also derive the magnitude of the upwelling from the third term in eq. (32), remembering that the x-variation of the upwelling itself is described by term (a) in eq. (33). It is most convenient to study eq. (32) at great depths. Since practically the whole z-variation takes place in the surface Ekman layer, $w\left(\overset{\circ}{x}, \infty, \overset{\circ}{t}\right) \cong w\left(\overset{\circ}{x}, \frac{\pi}{2}, \overset{\circ}{t}\right)$, that is, the upwelling velocity at great depths is about the same as the upwelling velocity at the bottom of the surface Ekman layer which I will call w_E^+. Thus we have from eq. (32),

$$(47) \quad w_E^+\left(\overset{\circ}{x}, \frac{\pi}{2}, \overset{\circ}{t}\right) = -\frac{D_z^2 \tau_y}{2 \pi^{3/2} \rho \nu_z D_x} \int_{\overset{\circ}{0}}^{\overset{\circ}{t}} \frac{\sin \sigma}{\sqrt{\sigma}} \cdot$$

$$\cdot \frac{4}{\sqrt{\pi \sigma}} \exp\left(\frac{-\overset{\circ}{x}^2}{\sigma}\right) \left(\int_{\overset{\circ}{0}}^{\infty} \exp\left(\frac{-\overset{\circ}{z}^2}{\sigma}\right) dz \right) d\sigma,$$

but

$$\int_{\overset{\circ}{0}}^{\infty} \exp\left(-\frac{\overset{\circ}{z}^2}{\sigma}\right) dz = \frac{1}{2} \sqrt{\pi \sigma}.$$

Therefore (47) becomes:

$$48) \quad w_E^+\left(\overset{\circ}{x}, \frac{\pi}{2}, \overset{\circ}{t}\right) = -\frac{D_z^2 \tau_y}{\pi^{3/2} \rho \nu_z D_x} \int_{\overset{\circ}{0}}^{\overset{\circ}{t}} \sin \sigma \, \frac{\exp\left(\frac{-\overset{\circ}{x}^2}{\sigma}\right)}{\sqrt{\sigma}} \, d\sigma$$

This is exactly eq. (35) (Fredholm's solution) multiplied by D_z/D_x except that the variable $\overset{\circ}{z}$ is replaced by $\overset{\circ}{x}$. It is therefore a Fredholm solution for the coastal Ekman layer which implies the Ekman solution and the w given above (It should be noted in this connection that the non-slip condition, $w\left(0, \overset{\circ}{z}, \overset{\circ}{t}\right) = 0$ is not satisfied by eq. (32). It was not needed to obtain eq. (32). Thus in the real world one would expect a thin adjustment layer at the coast, controlled by other equations than the rest of the system, within which w goes from its maximum value near the coast to 0 at the coast. Garvin (1971) showed that this adjustment layer is so thin as to have no effect whatsoever on the total upwelled volume).

Now we will investigate the order of magnitude for the third term of eq. (32) with the x-variation described by (b) of eq. (33). This as we remember describes the sinking caused by the convergence of the model wind.

First we note that for small $\overset{\circ}{\lambda}_2$ we have,

$$(49) \quad (b) = -2\overset{\circ}{\lambda}_2\left[\Phi\left(\frac{-\overset{\circ}{x}}{\sqrt{\sigma}}\right)+\Phi\left(\frac{\overset{\circ}{x}}{\sqrt{\sigma}}\right)\right]$$

Writing this out in complete form,

$$(50) \quad (b) = -2\overset{\circ}{\lambda}_2\frac{2}{\sqrt{\pi}}\left[\int_{\frac{-\overset{\circ}{x}}{\sqrt{\sigma}}}^{\infty}\exp(-x'^2)\,dx' + \int_{\frac{\overset{\circ}{x}}{\sqrt{\sigma}}}^{\infty}\exp(-x'^2)\,dx'\right]$$

Now since $\exp(-x^2)$ is an even function,

$$\int_{x}^{\infty}\exp(-x'^2)\,dx' = \int_{-\infty}^{-x}\exp(-x'^2)\,dx';$$

then (50) becomes

$$(51) \quad (b) = -2\overset{\circ}{\lambda}_2\frac{2}{\sqrt{\pi}}\left[\int_{-\infty}^{\infty}\exp(-x^2)\,dx'\right] = -4\overset{\circ}{\lambda}_2 .$$

In other words when $\overset{\circ}{\lambda}_2$ is small, the sinking takes place at the same rate for all $\overset{\circ}{x}$.

Now substituting this value into the third term of (39) we have for w_E^-, the speed of sinking at the bottom of the surface Ekman layer,

$$(52) \quad w_E^- = \frac{D_z^2\,\tau_y\,\overset{\circ}{\lambda}_2}{\pi^{3}/_{2}\,\rho\nu_z\,D_x}\int_{\overset{\circ}{0}}^{\overset{\circ}{t}}\sin\sigma\,d\sigma$$

or,

$$(53) \quad w_E^- = \frac{D_z^2\,\tau_y\,\overset{\circ}{\lambda}_2}{\pi^{3}/_{2}\,\rho\nu_z\,D_x}(1-\cos\overset{\circ}{t}) .$$

This describes a motion of inertial frequency $\frac{2\pi}{f}$ with a maximum downward speed of

$$w_{E\max}^- = \frac{2\,D_{z_2}\,\tau_y\,\overset{\circ}{\lambda}_2}{\pi^{3}/_{2}\,\rho\nu_z\,D_x} = 3\times 10^{-4}\ \text{cm/sec}$$

and an average speed over a pendulum day of 1.5×10^{-4} cm/sec downwards.

Thus the water that rises in the coastal Ekman layer sinks by continuity in a region of about 2000 km width uniformly (independent of x). The periodic character of this solution at the bottom of the Ekman layer corresponds to the dependence of the "convergence time" of Fredholm's solution on depth (EKMAN, 1905). Thus at great depths the above wave motion will practically always exist.

4.2. The Vertical Wave Amplitude is Determined

First of all the definition for u_r, the reference velocity in 4 is as follows:

$$u_r \equiv \frac{\tau_x}{2\sqrt{2}\,\rho\nu_z^{1/2}(2\Omega)^{1/2}}$$

where Ω is the rotational frequency of the earth.

In defining u_r and thus in determining the scale in figures 4, $f^{1/2}$ which appears in eqs. (39), (40), (43) and (44) as a part of D_z, has been split up into $(\sin\varphi)^{1/2}\cdot(2\Omega)^{1/2}$, that is a latitude-dependent part and a constant part.

With this,

$$u_r = 3.4 \text{ cm/sec.}$$

Thus at 20° N, as one can see from figure 4

$$u_1 = 13 \text{ cm/sec}$$
$$v_1 = 5 \text{ cm/sec.}$$

Thus at 20° N and about 50 km from shore, the elliptical motion described by the periodic terms of eqs. (41) and (42) would describe a displacement of isolines (isohalines, isotherms, etc.) of about 2.7 kilometers east-west and about 1.1 kilometers north-south each day.

Now in analogy to the treatment in section 4.1, we will consider the motion of the periodic terms within the coastal Ekman layer whose x-variation is described by (a) in eq. (33). If we again assume the vertical velocity w_{E1} at the bottom of the surface Ekman layer to be about the same as the vertical velocity deep in the ocean, we can write immediately in analogy to (47) from (32) and (33) with

$$\int_0^\infty \exp\left(-\frac{z'^2}{\sigma}\right) d\overset{\circ}{z}' = \frac{1}{2}\sqrt{\pi\sigma}$$

that,

$$(54)\quad w_{E1}\left(\overset{\circ}{x} < \frac{\pi}{2}, \frac{\pi}{2}, \overset{\circ}{t}\right) = -\frac{D^2_z\,\tau_y}{2\,\pi^{3/2}\,\rho\,\nu_z\,D_z}\left\{\sin\frac{\omega}{f}\overset{\circ}{t}\cdot\right.$$

$$\cdot\int_0^{\overset{\circ}{t}}\left[\cos\left(\frac{\omega}{f}+1\right)\sigma+\cos\left(\frac{\omega}{f}-1\right)\sigma\right]\frac{\exp\left(-\frac{\overset{\circ}{x}^2}{\sigma}\right)}{\sqrt{\sigma}}\,d\sigma-\cos\frac{\omega}{f}\overset{\circ}{t}\cdot$$

$$\left.\cdot\int_0^{\overset{\circ}{t}}\left[\sin\left(\frac{\omega}{f}+1\right)\sigma+\sin\left(\frac{\omega}{f}-1\right)\sigma\right]\frac{\exp\left(-\frac{\overset{\circ}{x}^2}{\sigma}\right)}{\sqrt{\sigma}}\,d\sigma.\right.$$

But (54) is just $-D_z/D_x$. (37). This will yield a solution for the vertical wave amplitude in the coastal Ekman layer below $z = D_z$ which differs only in magnitude from the one for the east-west wave amplitude in the surface Ekman layer outside of $x = D_x$. Indeed this corresponds with expectations: From continuity, water must come up in the coastal Ekman layer, when the periodic movement in the surface Ekman layer is directed away from shore and vice-versa.

In addition, the solution for $\overset{\circ}{t} \to \infty$ and for small $\overset{\circ}{x}$, will be just $-D_z D_x$. (39). Thus the curve on the right-hand side of fig. 4 describes as well the variation with latitude of the maximum vertical wave amplitude in the coastal Ekman layer in units of w_r, a reference velocity, where $w_r = 3.4 \times 10^{-3}$ cm/sec. At 20° N this maximum wave amplitude is then

$$w_{Emax}\left(\overset{\circ}{x} \ll \frac{\pi}{2}, \frac{\pi}{2}, \overset{\circ}{t} \gg 1 \right) = 1.3 \times 10^{-2} \text{ cm/sec.}$$

This will approach much larger values as 30° N is neared.

This whole development holds for $0 \leq \varphi < 30°$ N. One could extend it in a way similar to the treatment of the horizontal wave amplitudes for $\varphi > 30°$ N.

We can now investigate the amplitude of the vertical oscillations at the distance $x = D_x$ and at 20° N latitude whose x-variation is described by (a) in eq. (33). Making the same assumption that the vertical velocity at the bottom of the surface Ekman layer and at great depths are similiar, we have with w_{E_2} the vertical velocity at the bottom of the Ekman layer for this part of eq. (32),

$$(55)\quad w_{E_2}\left(\overset{\circ}{x} \geqslant \frac{\pi}{2}, \frac{\pi}{2}, \overset{\circ}{t} \right) = \frac{D_z^2 \tau_x \overset{\circ}{\lambda}_1}{2 \pi^{3/2} \rho \nu_z D_x} \left\{ \sin \frac{\omega}{f} \overset{\circ}{t} \cdot \right.$$

$$\cdot \int_0^{\overset{\circ}{t}} \left[\cos\left(\frac{\omega}{f} + 1 \right)\sigma + \cos\left(\frac{\omega}{f} - 1 \right)\sigma \right] d\sigma - \cos \frac{\omega}{f} \overset{\circ}{t} \cdot$$

$$\left. \cdot \int_0^{\overset{\circ}{t}} \left[\sin\left(\frac{\omega}{f} + 1 \right)\sigma + \sin\left(\frac{\omega}{f} - 1 \right)\sigma \right] d\sigma \right.,$$

with the assumption that at $\overset{\circ}{x} = \frac{\pi}{2}$, $\overset{\circ}{\lambda}_1 = 7 \times 10^{-2}$ is small enough to neglect the x-variation as shown in the last section.

(55) can be written with $a = \frac{\omega}{f}$,

$$(56)\quad w_{E_2}\left(\overset{\circ}{x} \geqslant \frac{\pi}{2}, \frac{\pi}{2}, \overset{\circ}{t} \right) = \frac{D_z^2 \tau_x \overset{\circ}{\lambda}_1}{2 \pi^{3/2} \rho \nu_z D_x} \left\{ \sin a\overset{\circ}{t} \cdot \right.$$

$$\cdot \left[\frac{1}{a+1} \sin (a+1)\overset{\circ}{t} + \frac{1}{a-1} \sin (a-1)\overset{\circ}{t} \right] - \cos a\overset{\circ}{t} \cdot$$

$$\left. \left[\frac{1 - \cos (a+1)\overset{\circ}{t}}{a+1} + \frac{1 - \cos (a-1)\overset{\circ}{t}}{a-1} \right] \right\} .$$

With the help of trigonometric identities, (56) can be written:

$$(57)\quad w_{E2}\left(x \geqslant \frac{\pi}{2}, \frac{\pi}{2}, \overset{\circ}{t}\right) = \frac{D_z^2 \tau_x \overset{\circ}{\lambda}_1}{4 \pi^{3}/_{2} \rho \nu_z D_x} \cdot \cdot \left[\frac{2a}{a^2 - 1}\right][2 \cos \overset{\circ}{t} - \cos a \overset{\circ}{t}] \quad .$$

This describes the interference of two waves, the first with the inertial frequency and the second with the frequency of $2\pi/1$ day. The inertial frequency results from the infinitely-slow convergence to a steady state at great depths, similiar to w_E of the last section. The maximum value of w_{E2} by 20° N then would be,

$$w_{E2\,max}\left(\overset{\circ}{x} \geqslant \frac{\pi}{2}, \frac{\pi}{2}, \overset{\circ}{t}\right) = \frac{D_z^2 \tau_x \lambda_1}{4 \pi^{3}/_{2} \rho \nu_z D_x}\left[\frac{3}{1{,}25}\right][3] = 1.2 \times 10^{-3} \text{ cm/sec}$$

By 30° N as one would expect from eq. (57), this effect becomes larger.

5. Conclusions

In the introduction several explainations for the spacial variation of upwelling were given, leaving the third possibility at the end to be discussed later. In the meantime, we have shown analytically (eqs. (41), (42), (45) and (46) that a resonance point exists at 30° N) where the amplitudes of the wave motion approaches infinity mathematically. But what happens in the real world?

Clearly as we approach nearer and nearer to 30° N the assumption of $\frac{\partial}{\partial y} = 0$ no longer holds. It is indeed a bit of a paradox that we set $\frac{\partial}{\partial y} = 0$ at the beginning and get an variation of the amplitudes of the periodic terms with latitude caused by the variation of f. We have considered however the effect of a local wind on the velocity field and locally f = constant is a good approximation. We can then in effect solve for different points along a coast which have different values of f, values which are constant around the points themselves. We can then take more and more points, until we have a continuous representation of the velocity field.

As we approach 30°, the non-linear advection terms grow to be as important as the other terms in eq. 1. This is so for instance when $\frac{\partial v}{\partial y} = f = 7 \times 10^{-5}$. This corresponds to a change in velocity of 10 cm/s in 1,4 km. The study of fig. 5 shows that this gradient is reached only very near to 30° N and emphasises the narrowness of this effect. Thus other terms in the equation become important by 30° N and have a "damping" effect on the growth of the amplitudes. But where does the increased energy by 30° N go? There seem to be two possible answers to this question.

One could assume that this increased energy is transformed by non-linear exchanges to the mean velocity field. This might be an attractive way to try to get an increased upwelling intensity at 30° N. This seems to me to be a dilettantish approach: to work with a linear model and then suddenly explain one of the main effects one hopes to explain by sticking on some catch-all, non-linear effects at the end.

It seems more logical and in the sense of the damping phenomena that this increased energy is fed into the turbulent velocity field. Studies of turbulence spectrum have shown, (Phillips, 1966), that the input of energy into the turbulent field takes place

at small wave numbers (large wave lengths). A typical value for an input wave number into the vertical turbulence (which is of the most interest here) would be $1/D_z$. This would correspond to a vertical movement of 50 m in 12 hours or 1×10^{-1} cm/sec. for the ware motions derived here.

From fig. 4 and the value of the reference wave amplitude, w_r, for the coastal Ekman layer, one sees that this value is reached at about 29° N and grows larger up to 30° N. About the same holds for the other side of 30° N. The increased mixing in this narrow zone has no immediate effect of increasing the nutrient-supply: In the coastal zone, with the wind field given, the water that is mixed would be upwelling anyway without the mixing. But this increased mixing could have important secondary effects on the biology of the area, a problem requiring a biologist's analysis. In addition if the trade winds should weaken or break down for a particular time period, the increased mixing induced in this narrow region by the seabreeze-landbreeze (which in general at least off the coast of Northwest Africa should be present) would have the primary effect of introducing nutrients into the uppermost ocean layers.

On the other hand by examining eq. (57) for the vertical wave motion at $x \geqslant D_x$, one sees that the vertical wave amplitude reaches the value of 1×10^{-1} cm/sec by about 29°40′ N, that is, very close to 30° N (again about the same on the other side of 30° N). In this narrow region the increased turbulence would lead to increased mixing, having the effect of bringing cooler, nutrient-richer water into the surface layers. This proposed local maximum of temperature and nutrient-concentration for $x \geqslant D_x$ confined as it is to a width of about 1° latitude, is too narrow to be shown on most large scale property-distribution maps available.

Therefore at 30° N, one would expect no extra upwelling in the sense of the definition at the beginning, at least not from this linear theory, but the increased mixing will have effects similar to those of upwelling. This result could thus explain the local temperature minimum at 30° S off the coast of Chile as shown in fig. 1. If the seabreeze-landbreeze is a more or less constant feature at 30° N, it should be possible to check this prediction by making a series of closely spaced stations perpendicular to 30° from about 25° N to 35° N, measuring at best the nutrient concentration or perhaps the turbidity.

It would seem possible to extend this theory analytically to an ocean of finite depth. Then a combination of the two cases with appropriate boundary conditions could describe the upwelling in an ocean with a shelf and perhaps give some indications as to the variation of upwelling intensity with the width and depth of the shelf. It would also be of interest to numerically evaluate the results obtained for the general velocity field. In this way the time development of the individual terms could be studied, and a more detailed picture of the motion would be given in the end.

Acknowledgements

I am indebted to the late Prof. G. DIETRICH for overseeing my work and especially thank Dr. M. TOMCZAK, with whom I have had many fruitful discussions concerning upwelling in general and the development and the results of the theory dealt with in this paper in particular.

In addition I would like to thank my wife, Heidi, who lightened my burden by doing most of the typing.

Bibliography

ARTHUR, R. S. (1965): On the calculation of vertical motion in eastern boundary currents from determinations of horizontal motion. J. geophys. Res. **70**, 2799—2803.

EKMAN, V. W. (1905): On the influence of the earth's rotation on ocean-currents. Ark. Matem. Astronom. och Fysik. **2**, 1—53.

GARVINE, R. W. (1971): A simple model to the theory of upwelling and coastal dynamics. J. phys. Oceanography **1**, 169—179.

HIDAKA, K. (1954): A contribution to the theory of upwelling and coastal currents. Transact. amer. Geophys. Union. **35**, 431—444.

KRAUSS, W.: Methoden und Ergebnisse der theoretischen Ozeanographie. I. Dynamik des homogenen und quasihomogenen Meeres. Stuttgart, Borntraeger (in press).

MARKGRAF, H. (1955): Die vorherrschenden Winde auf dem Atlantischen Ozean im Januar und Juli. Deutscher Wetterdienst, Seewetteramt Hamburg, Einzelveröentl. **7**.

MARKGRAF, H. (1960) Die vorherrschenden Winde auf dem Atlantischen Ozean im April und Oktober. Deutscher Wetterdienst, Seewetteramt Hamburg, Einzelveröfftl. **25**.

PHILLIPS, O. M. (1966): The dynamics of the upper ocean. Cambridge, Cambridge University Press.

SAITO, Y. (1956): Theory of the transient state concerning upwelling and coastal currents. Transact. amer. Geophys. Union **37**, 38—42.

SMITH, R. L. (1968): Upwelling. Oceanogr. Mar. Biol. Ann. Rev. **6**, 11—46.

TOMCZAK, M. jr. (1970): Eine lineare Theorie des stationären Auftriebs im stetig geschichteten Meer. Dt. Hydrograph. Zeitschr. **23**, 214—234.

TOMCZAK, M. jr. (1973): An investigation into the occurance and development of cold water patches in the upwelling region of N.W. Africa. (In preparation; to be published in: Meteor-Forschungsergebnisse A.)

VOORHIS, A. D. (1968): Measurements of vertical motion and the partition of energy in the New England slope water. Deep Sea Res. **15**, 599—608.

WOOSTER, W. S. (1970): Auftrieb und der Peru Strom. In: Erforschung des Meeres. Hrsg. v. G. Dietrich. Umschau, Frankfurt. 39—51.

WOOSTER, W. S. and REID, jr. J. L. (1963): Eastern boundary currents. In: The Sea. Ed. by M. N. Hill, Wiley, New York, **II**. 253—280.

WYRTKI, K. (1964): The thermal structure of the eastern tropical Pacific Ocean. Dt. Hydrograph. Zeitschr. Suppl. Ser A (8°) **6**, 84ff.

YOSHIDA, K. (1967): Circulation in the eastern tropical oceans with special references to upwelling and under-currents. Jap. J. Geophys. **4**, 1—75.